Biochem. J. (2013) **454**, 411–416 (Printed in Great Britain) doi:10.1042/BJ20130550

Chemical suppression of an oncogenic splicing variant of AIMP2 induces tumour regression

Hee Sook LEE*[1], Dae Gyu KIM*[1], Young Sun OH*†[1], Nam Hoon KWON*, Jin Young LEE*, Doyeun KIM*, Song-Hwa PARK*, Jong-Hwan SONG‡, Sunkyung LEE‡, Jung Min HAN*, Bum-Joon PARK§, Jongkook LEE‖ and Sunghoon KIM*¶[2]

*Medicinal Bioconvergence Research Center and College of Pharmacy, Seoul National University, Seoul 305-343, Korea, †Department of Biological Science and the Basic Science Research Institute, Sungkyunkwan University, Suwon 151-742, Korea, ‡Bio-Organic Science Division, Korea Research Institute of Chemical Technology, Daejeon 440-746, Korea, §Department of Molecular Biology, College of Natural Science, Pusan National University, Busan 609-735, Korea, ‖College of Pharmacy, Kangwon National University, Chuncheon, Gangwon 200-701, Korea, and ¶Department of Molecular Medicine and Biopharmaceutical Sciences and Graduate School for Convergence Technologies, Seoul National University, Seoul 151-742, Korea

AIMP2 (aminoacyl-tRNA synthetase-interacting multifunctional protein 2) is a potent tumour suppressor that induces apoptosis in response to various oncogenic signals. AIMP2-DX2, an exon2-deleted splicing variant of AIMP2, is up-regulated in lung cancer and competitively suppresses the pro-apoptotic activity of AIMP2, resulting in tumorigenesis. In the present study we report that BC-DXI01, a synthetic compound, specifically reduces the cellular levels of AIMP2-DX2 through selective degradation of the AIMP2-DX2 mRNA transcript. We found that BC-DXI01-mediated cell death positively correlates with AIMP2-DX2 expression in the lung cancer cell lines tested. Administration of BC-DXI01 in a AIMP2-DX2-driven tumour xenograft mice model led to reduced tumour sizes and volumes of up to 60 % in comparison with vehicle-treated mice group, consistent with decreases in AIMP2-DX2 transcript and protein levels. Taken together, our findings suggest that tumorigenic activity of AIMP2-DX2 can be controlled by the small chemical BC-DXI01, which can selectively suppress the AIMP2-DX2 mRNA transcript.

Key words: aminoacyl-tRNA synthetase-interacting multifunctional protein 2 (AIMP2)-DX2, chemical suppression, lung cancer, mRNA, splicing variant.

INTRODUCTION

ARSs (aminoacyl-tRNA synthetases) are essential enzymes for protein synthesis, conjugating amino acids to their cognate tRNAs. In higher eukaryotes, nine different ARSs form a MSC (multi-tRNA synthetase complex) comprising non-enzymatic factors and AIMPs (ARS-interacting multifunctional proteins) [1]. The three AIMPs, AIMP1/p43, AIMP2/p38 and AIMP3/p18, function as scaffolding proteins for the assembly and integrity of the MSC. However, they are capable of dissociating from the MSC whereupon they participate in various regulatory pathways [1].

Among the AIMPs, AIMP2, which consists of four exons, is a potent tumour suppressor, which triggers growth-arrest signalling of TGF-β (transforming growth factor-β). This growth-arrest signalling occurs by its enhancement of ubiquitin-mediated degradation of FBP (FUSE-binding protein), which is a transcriptional activator of the proto-oncogene Myc [2]. In addition, upon TNF-α (tumour necrosis factor-α) stimulation, AIMP2 induces cell apoptosis by facilitating ubiquitination of TRAF2 (TNF-receptor-associated factor 2) [3]. AIMP2 also reinforces pro-apoptotic signalling by protecting the tumour suppressor p53 from MDM2 (murine double minute 2)-mediated degradation under DNA damage stress [4]. The anti-proliferative and pro-apoptotic roles of AIMP2 have been supported by an *in vivo* mouse model, whereby *Aimp2*-heterozygous mice, as compared with wild-type mice, were shown to be more vulnerable to tumorigenesis in lung, colon and skin carcinogenesis xenograft models [5].

Interestingly, AIMP2-DX2, an isoform of AIMP2 in which exon2 is deleted by alternative splicing, has been detected in cancer cell lines and tissues [6]. Like AIMP2, AIMP2-DX2 binds to FBP, TRAF2 and p53; however, it competes with AIMP2 for binding to these target proteins, consequently inhibiting the tumour-suppressive roles of AIMP2 [6,7]. The expression ratio of AIMP2-DX2 to AIMP2 positively correlates with the malignancy of lung cancers in patients, as well as chemoresistance of ovarian cancer [6,7]. These data suggest that AIMP2-DX2 might be an attractive target for developing cancer therapeutics.

Lung cancer is one of the most frequently occurring cancer types in humans, and is the leading cause of cancer-related death worldwide [8]. The need for an effective anti-lung cancer drug is obvious; however, current lung cancer treatment is principally dependent on cytotoxic drugs. Only a few targeted drugs are available to treat lung cancer due to the poor understanding of the mechanism of lung carcinogenesis, and, as a result, effective targets are scarce [9]. Since the expression of AIMP2-DX2 adversely affects lung cancer progression and patient survival [6], inhibitors of AIMP2-DX2 expression may prove effective therapeutic agents for lung cancer. Indeed, knockdown of AIMP2-DX2 in a lung cancer mouse model by RNAi has been shown to significantly suppress tumorigenesis in the lung [6]. However, an effective small-molecule inhibitor of AIMP2-DX2 has not yet been reported. In the present paper we report that a small molecule

Abbreviations used: ARS, aminoacyl-tRNA synthetase; AIMP, ARS-interacting multifunctional protein; AIMP2-F, full-length AIMP2; FBP, FUSE-binding protein; IHC, immunohistochemistry; MDM2, murine double minute 2; MSC, multi-tRNA synthetase complex; NSCLC, non-small-cell lung cancer; RT, reverse transcription; TNF, tumour necrosis factor; TRAF2, TNF-receptor-associated factor 2.

[1] These authors contributed equally to this work.

[2] To whom correspondence should be addressed (email sungkim@snu.ac.kr).

termed BC-DXI01 specifically inhibits the expression of AIMP2-DX2 through down-regulation of its mRNA transcript, and we show the molecule has anti-tumorigenic activity in an *in vivo* mouse model.

EXPERIMENTAL

An expanded Experimental section is available in the Supplementary Online Information (at http://www.biochemj.org/bj/454/bj4540411add.htm).

Compounds

A total of 2231 small compounds were sorted from ChemDiv's synthetic chemical library to maximize the coverage of structural diversity. To prepare BC-DXI01, ethyl 3-chloro-3-oxopropanoate (13.4 g, 0.089 mol) and triethylamine (1.25 ml, 0.089 mol) were added to a mixture of 4-aminobenzoic acid (10.0 g, 0.073 mol) in acetone (200 ml). The reaction mixture was stirred at room temperature (25 °C) for 4 h, and all volatiles were removed under reduced pressure. The residue was dissolved in water and acidified to pH 3 with concentrated HCl, the resulting precipitates were filtered and collected as an off-white solid (13.0 g, 75 % yield): ^{1}H-NMR (DMSO-d_6, 300 MHz): δ 12.72 (s, 1 H), 10.46 (s, 1 H), 7.88 (d, 1 H, *J* 8.7 Hz), 7.65 (d, 1 H, *J* 8.7 Hz), 4.10 (q, 2 H, *J* 7.2 Hz), 3.47 (s, 2 H), 1.17 (t, 3 H, *J* 7.2 Hz). For biotinylation of BC-DXI01, a mixture of BC-DXI01 (25.0 mg, 0.10 mmol), amine–PEG_2–biotin (37.1 mg, 0.10 mmol), EDCI [1-ethyl-3-(3-dimethylaminopropyl)carbodiimide] (28.5 mg, 0.15 mmol), hydroxybenzotriazole (20.1 mg, 0.15 mmol) and triethylamine (41.4 μl, 0.30 mmol) in anhydrous DMF (dimethylformamide) was stirred for 48 h at room temperature. The mixture was diluted with water (1 ml) and extracted with dichloromethane (3× 20 ml). The combined organic layer was washed with brine, dried over anhydrous sodium sulfate and concentrated *in vacuo*. The residue was purified by flash-column chromatography on silica gel (hexanes/ethyl acetate, 1:2) to give the biotinylated BC-DXI01 (11.0 mg, 20 %) as a white solid: ^{1}H-NMR [trichloro(^{2}H)methane, 300 MHz]: δ 9.44 (s, 1 H), 8.03 (d, *J* 6.4 Hz, 2 H), 7.60 (t, *J* 8.1 Hz, 2 H), 7.37 (t, *J* 8.3 Hz, 2 H), 7.29 (d, *J* 2.3 Hz, 2 H), 4.28 (quintet, *J* 7.6 Hz, 2 H), 3.52–3.48 (m, 2 H), 3.38–3.23 (s, 2 H), 2.97 (d, *J* 7.9 Hz, 6 H), 2.90 (d, *J* 7.7 Hz, 6 H), 1.39–1.07 (m, 13 H); MS (ES +) *m/z* calculated for $C_{28}H_{41}N_5O_8S$ (M^+) 607.2, found 607.0. For the synthesis of BC-DXI01-Na salt, the benzoic acid (4.7 g, 20 mM) was dissolved in hot ethanol (80 ml). To the solution 10 M NaOH (2 ml) was added, and the mixture was stood at room temperature. The precipitates were filtered and collected as an off-white solid (4.2 g, 81 % yield): ^{1}H-NMR (^2H_2O, 300 MHz): δ 7.71 (d, 1 H, *J* 8.4 Hz), 7.36 (d, 1 H, *J* 8.4 Hz), 4.57 (q, 2 H, *J* 6.3 Hz), 3.44 (s, 2 H), 1.11 (t, 3 H, *J* 7.2 Hz).

Small compound screening based on the luciferase assay

The AIMP2-DX2 gene was cloned into the pGL2 control vector by HindIII digestion to generate luciferase-tagged protein. pGL2-AIMP2-DX2 was transfected into cell lines using Fugene HD (Roche), according to the manufacturer's instructions. After a 12 h incubation, cells were counted and seeded into 96-well plates (10^4 cells/well) and incubated for 12 h. A total of 2231 small compounds (ChemDiv) dissolved in DMSO were added to the pGL2-AIMP2-DX2-transfected H460 cell lines at a 10 μM concentration in serum-free medium. After a 4-h incubation, cells were lysed and analysed using a firefly luciferase assay system (Promega) to detect luminescence. The compounds which showed an over 40 % decrease in the luminescence of AIMP2-DX2 compared with the DMSO control were chosen. Selected compounds were further tested to monitor the cytotoxicity based on the MTT assay using WI-26 normal lung cells.

RT (reverse transcription)–PCR

Total RNA was isolated from cell lines or frozen tumour tissues using TRIzol® (Invitrogen) and converted into cDNAs using Moloney murine leukaemia virus reverse transcriptase (Invitrogen) and random hexamers according to the manufacturer's guidelines. PCRs were performed with PCR master mix (Bioneer) using primer pairs of 5′-ATGCCGATGTACCAGGTAAAG-3′ (forward) and 5′-CTTAAGGAGCTTGAGGGCCGT-3′ (reverse) for the simultaneous detection of both AIMP2-F (full-length AIMP2) transcript (960 bp) and AIMP2-DX2 transcript (753 bp). The primers 5′-CTGGCCACGTGCAGGATTACGGGG-3′ (forward) and 5′-AAGTGAATCCCAGCTGATAG-3′ (reverse), were used to specifically detect AIMP2-DX2 transcript (231 bp). The β-actin gene was used as an internal control, and was amplified using the primer set of 5′-CCTTCCTGGGCATGGAGTCCT-3′ (forward) and 5′-GGAGCAATGATCTTGATCTT-3′ (reverse) generating a 202 bp PCR product. PCRs were carried out using the PCR thermocycler (TaKaRa) under the following conditions: initial denaturation at 94 °C for 2 min, 33 (for simultaneous detection of both AIMP2-F and AIMP2-DX2 transcripts) or 30 (for single AIMP2-F gene detection) cycles of amplification (denaturation at 94 °C for 30 s, annealing at 60 °C for 30 s and extension at 72 °C for 45 s), and extension at 72 °C for 5 min. The PCR products were electrophoresed on a 1.5 % agarose gel and stained with ethidium bromide.

Xenograft mice model

Animal experiments complied with the University Animal Care and Use Committee guidelines at Seoul National University. The tumour mass was obtained by subcutaneous injection of H460 cell lines in 5-week-old BALB/c Slc-*nu* SP nude male mice. Tumour mass was extracted and dissected to 3 mm × 3 mm × 3 mm fragments and subcutaneously transplanted into healthy mice using a trocar and allowed to grow. When the tumour mass volume reached 80–117 mm^3, mice were divided into control and treatment groups ($n = 8$ per group), and vehicle or BC-DXI01 (50 mg/kg) was introduced via intraperitoneal (4 days) and intrasubcutaneous (24 days) injections. The vehicle was prepared by mixing 10 % DMSO and 90 % mixture (Tween 80/PEG 400/distilled water, 16:4:25, by vol.). Mice were monitored every day and tumour volumes and body weights were checked two times a week. After killing the mice, tumour weights were measured and subjected to IHC (immunohistochemistry).

RESULTS

Identification of compounds which reduce the cellular AIMP2-DX2 level

Since AIMP2-DX2 was previously suggested as a novel therapeutic target against NSCLC (non-small-cell lung cancer) [6], we set up the firefly luciferase assay system to screen a chemical library (2231 chemicals) for small molecules that inhibit the cellular level of AIMP2-DX2 (see Supplementary Figure S1 at http://www.biochemj.org/bj/454/bj4540411add.htm). In the screening system, H460 cells were transfected with pGL2-AIMP2-DX2 to express luciferase-tagged AIMP2-DX2 and four compounds were identified to reduce

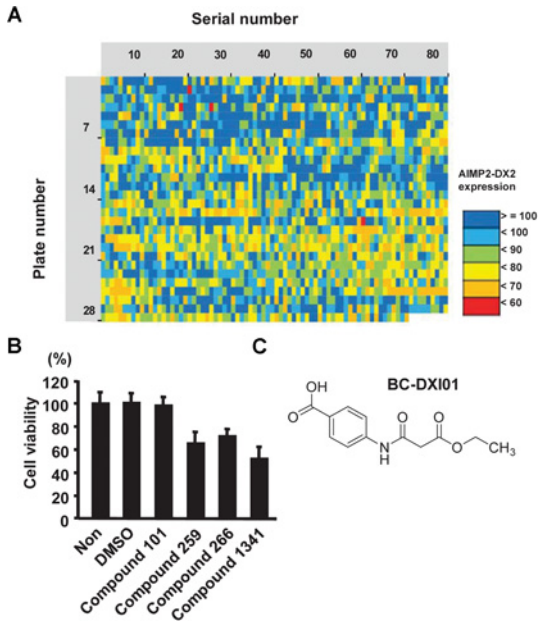

Figure 1 Identification of small chemicals which suppress the AIMP2-DX2 level

(**A**) Heat map of the primary screening data. Inhibitory effects of 2231 chemicals on the AIMP2-DX2 level were examined by luciferase reporter assay and the results are presented. Compounds 101, 259, 266 and 1341 which suppressed over 40 % of the AIMP2-DX2 level (red colour) were selected. (**B**) WI-26 cells were treated with the four compounds selected (10 μM) for 48 h to determine their cytotoxicity using the MTT assay. Results are means $\pm$ S.D. This experiment was repeated three times. Non, no addition. (**C**) Chemical structure of BC-DXI01.

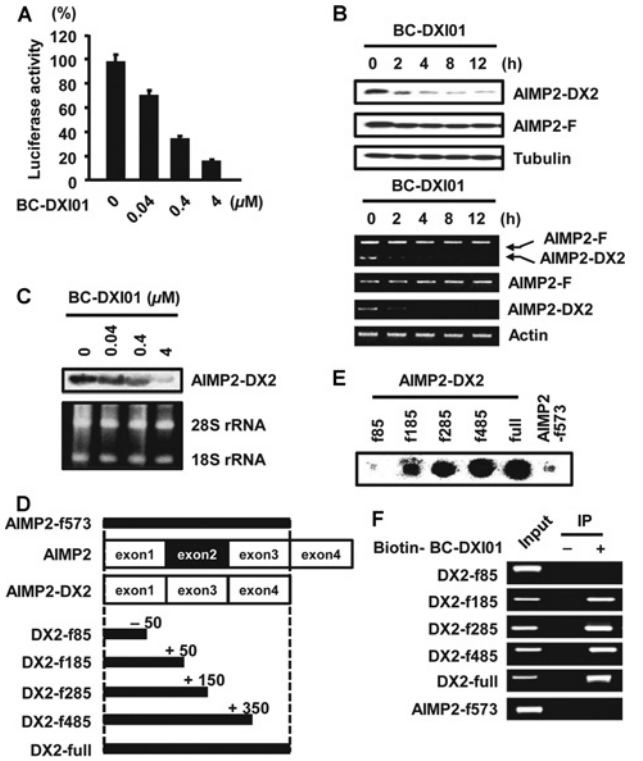

Figure 2 The effect of BC-DXI01 on the AIMP2-DX2 transcript level

(**A**) Dose-dependent effect of BC-DXI01 on the AIMP2-DX2 level using a luciferase assay. Results are means $\pm$ S.D. This experiment was repeated three times. (**B**) Protein and transcript levels (upper and lower panels respectively) of AIMP2-DX2 and AIMP2-F were monitored by immunoblotting and RT–PCR respectively, after 0.4 μM BC-DXI01 treatment for 12 h. (**C**) Mature mRNA of the AIMP2-DX2 transcript was detected by Northern blotting using an AIMP2-DX2-specific probe. (**D**) Schematic diagram of the RNA fragments that were prepared by *in vitro* transcription for the binding assay with BC-DXI01. (**E**) Each RNA fragment was radioactively synthesized using [α-^{32}P]UTP, and mixed with biotinylated BC-DXI01. The mixture was subjected to a filter-binding assay using streptavidin-coated membrane and the bound RNA was detected via autoradiography. (**F**) Each RNA fragment synthesized by *in vitro* transcription was mixed with biotinylated BC-DXI01, and pulled down (IP) using streptavidin beads. RNA was purified from the captured complex and detected via RT–PCR using specific primer pairs.

cellular levels of AIMP2-DX2 by over 40 % compared with control (Figure 1A). Those included compound 101, 4-[(3-ethoxy-1,3-dioxoprophyl)amino]-benzoic acid; compound 259, phenol, 4-{[bis(2-hydroxyethyl)amino]methyl}-2,6-bis(1,1-dimethylethyl); compound 266, 2,6-pyridinedicarboxylic acid, 2,6-bis[1-methyl-2-(1-methylethoxy)-2-oxoethyl] ester; and compound 1341, 1*H*-indene-1,3(2*H*)-dione, 2-(1,3-dihydro-3-oxo-2*H*-indol-2-ylidene). A further round of screening was performed using the MTT assay to select chemicals without cytotoxic activity against the normal lung cell line (Figure 1B). From this assay, compound 101 {4-[(3-ethoxy-1,3-dioxoprophyl)amino]-benzoic acid, CAS number 130217-49-1} (designated as BC-DXI01) was selected as the primary hit for further investigation (Figure 1C).

Specific suppression of the AIMP2-DX2 transcript by BC-DXI01

To examine the concentration-dependent inhibitory effect of BC-DXI01 on the AIMP2-DX2 level, 0.04, 0.4 and 4 μM BC-DXI01 or DMSO only were added to H460 cells transfected with pGL2-AIMP2-DX2. BC-DXI01 effectively reduced AIMP2-DX2 expression on the basis of luminescence (Figure 2A). The effect of BC-DXI01 on endogenous AIMP2-DX2 protein was also analysed by immunoblotting, and the same result was observed (see Supplementary Figure S2A at http://www.biochemj.org/bj/454/bj4540411add.htm). Since 0.4 μM BC-DXI01 provided a robust suppressive effect, we used 0.4 μM for additional experiments. Next, we monitored the duration of efficacy by treating H460 cells with BC-DXI01 for the indicated times and analysed the levels of AIMP2-DX2 by immunoblotting (Figure 2B, upper panel). The AIMP2-DX2 level decreased significantly within 2 h, and decreased progressively to an almost undetectable level within 12 h after treatment. BC-DXI01 did not affect the cellular level of AIMP2-F, indicating that BC-DXI01 specifically suppresses AIMP2-DX2.

To see whether BC-DXI01 influences the level of the AIMP2-DX2 mRNA transcript, total RNA was extracted from the H460 cells, and the AIMP2-F and AIMP2-DX2 mRNA levels were analysed using RT–PCR with primer pairs which could simultaneously detect both AIMP2-F and AIMP2-DX2 transcripts. Interestingly, levels of the AIMP2-DX2 transcript were decreased from 2 h after BC-DXI01 treatment and continuously reduced as shown for AIMP2-DX2 protein levels. However, levels of the AIMP2-F transcript were unchanged by BC-DXI01 treatment (Figure 2B, lower panel, top gel). PCR cycles were reduced to detect AIMP2-F only without saturation and the same result was observed (Figure 2B, lower panel, upper middle gel). The effect of BC-DXI01 on the AIMP2-DX2 transcript was confirmed using the AIMP2-DX2-specific primers and the result showed that, unlike AIMP2-F, AIMP2-DX2 expression was specifically reduced by BC-DXI01 treatment (Figure 2B, lower panel, lower middle gel). The reduction in the AIMP2-DX2 transcript level was observed from 30 min after chemical treatment, and steadily declined thereafter (see

Supplementary Figure S2B). When transcription was blocked by actinomycin D treatment, the degradation of AIMP2-DX2 mRNA was accelerated by BC-DXI01, showing a comparatively rapid reduction in AIMP2-DX2 mRNA compared with that of the actinomycin D-untreated cells (see Supplementary Figure S2C).

Since AIMP2-DX2 is an alternative splicing variant of AIMP2, we examined whether BC-DXI01 modulates the splicing of AIMP2-DX2. As a control, we transfected H460 cells with the pGINT plasmid, which comprises a splicing cassette capable of reporting alternative splicing by the expression of GFP [10]. We also transfected the pGINT-exon2 and pGINT-exon2-A152G plasmids [6], which are used for the monitoring of AIMP2-DX2-specific splicing. The fluorescence of GFP observed by the transfection of pGINT, pGINT-exon2 and pGINT-exon2-A152G was not affected by the treatment of BC-DXI01, suggesting that it is the mature mRNA transcript of AIMP2-DX2, but not the splicing process, that is the target of BC-DXI01 (see Supplementary Figure S2D).

To test whether BC-DXI01 modulates the cellular level of mature AIMP2-DX2 mRNA, we designed a DNA hybridization probe which specifically recognizes the exon1–3 junction sequence of the mature AIMP2-DX2 transcript, and examined AIMP2-DX2 mRNA levels by Northern blotting. We observed reduced levels of mature AIMP2-DX2 transcript after BC-DXI01 treatment (Figure 2C). Taken together, these results suggest that the decrease in AIMP2-DX2 protein by BC-DXI01 is due to BC-DXI01-mediated degradation of the mature AIMP2-DX2 transcript.

To understand the mechanism of BC-DXI01-mediated degradation of the mature AIMP2-DX2 transcript, we synthesized RNA fragments of AIMP2 or the AIMP-DX2 transcript via *in vitro* transcription (Figure 2D) and examined the binding affinity of BC-DXI01 to each RNA fragment using a filter-binding assay. BC-DXI01 showed apparent association with the fragments of AIMP2-DX2 transcripts which contain the exon1–3 junction sequence. However, this association was not observed in DX2-f85 and AIMP2-f573, which lacked the exon1–3 junction sequence (Figure 2E). We confirmed interaction between BC-DXI01 and the RNA fragments with the exon1–3 junction sequence by pulling down the compound–RNA complex and performing RT–PCR (Figure 2F). Since BC-DXI01 specifically bound to AIMP2-DX2 RNA fragments with the exon1–3 junction sequence, we suggest that BC-DXI01-mediated degradation of the mature AIMP2-DX2 transcript may be induced by the direct binding of BC-DXI01 to the region spanning the exon1–3 junction of the AIMP2-DX2 transcript.

Effect of BC-DXI01 on lung cancer cells

To examine the effect of AIMP2-DX2 inhibition on the viability of lung cancer cells, H460 cells were treated with BC-DXI01 and harvested at 24, 48 and 72 h. Using the MTT assay, we found that cell death was proportional to the dosage and duration of BC-DXI01 treatment, with 40 % of treated cells viable at the maximal dosage of 4 μM and duration of 72 h of treatment while cell viability was maintained at nearly 100 % in the control group (Figure 3A). BC-DXI01-induced cell apoptosis was also confirmed by flow cytometry-based cell cycle analysis, which showed a dose-dependent increase in the sub-G_1 fraction (Figure 3B). In addition, we found that, in BC-DXI01-treated H460 cells, active caspase 3, a marker of apoptosis, was present in levels proportional to the concentration of BC-DXI01 treatments (Figure 3C). We also found that active caspase 3 levels were inversely correlated with expression of PARP-1 [poly(ADP-ribose) polymerase 1], a cell proliferation marker, and AIMP2-DX2 (see Supplementary Figure S3 at http://www.biochemj.org/bj/454/bj4540411add.htm). Furthermore, a thymidine incorporation assay showed BC-DXI01 mediated inhibition of H460 cell proliferation (Figure 3D). Taken together, these data suggest that BC-DXI01 inhibits the anti-apoptotic and pro-proliferative effects of AIMP2-DX2.

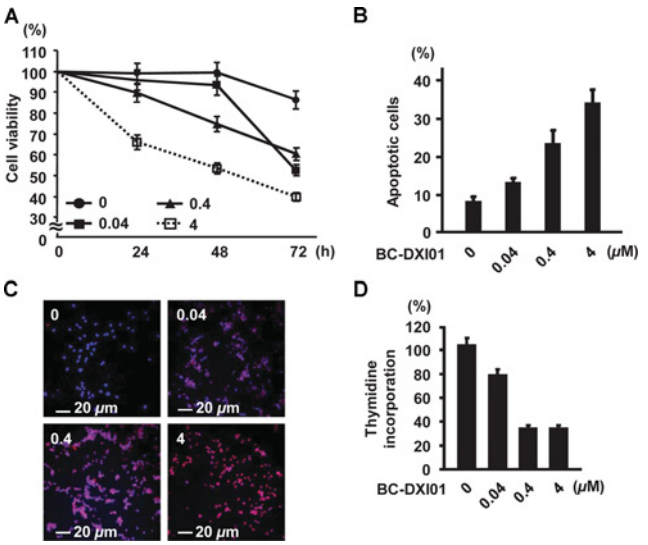

Figure 3 Effect of BC-DXI01 on apoptosis of H460 lung cancer cells

(**A**) H460 cells treated with BC-DXI01 were harvested at the indicated time points and the cell viability was measured using the MTT assay. (**B**) Cell cycle of H460 cells treated with BC-DXI01 for 48 h was analysed using flow cytometry. BC-DXI01-induced apoptosis was determined by monitoring the sub-G_1 population. (**C** and **D**) H460 cells were treated with the indicated concentrations of BC-DXI01 for 48 h. Cells were stained with anti-(active caspase 3) antibody (red) and DAPI (nucleus, blue), and the immunofluorescence images were merged (**C**). Cell proliferation of BC-DXI01-treated H460 cells was measured using a [^{3}H]thymidine incorporation assay (**D**). Values in (**A**), (**B**) and (**D**) are means $\pm$ S.D, and all of these experiments were repeated three times.

Positive correlation between AIMP2-DX2 levels and the pro-apoptotic activity of BC-DXI01

To determine the effects of BC-DXI01 in various NSCLC cell lines, and also to see whether its effect is affected by AIMP2-DX2, we analysed the cellular levels of AIMP2-DX2 in ten NSCLC cell lines, and compared them with that of the normal lung cell line WI-26. First, we found that, in BC-DXI01-untreated cell lines, H1972 and H1171 cells expressed similar levels of AIMP2-DX2 protein as the control, whereas the other eight lung cancer cell lines expressed higher than normal levels of AIMP-DX2 protein (Figure 4A, top panel). We then tested the effects of BC-DXI01 treatment, and found an obvious reduction in AIMP2-DX2 levels in all of the cancer cell lines, except for H1972 and H1171 cells in which AIMP2-DX2 levels were intrinsically low. Whereas AIMP2-DX2 levels varied to some small degree between the tested cell lines, AIMP2-F levels were not affected by BC-DXI01 treatment (Figure 4A, middle gels). A cell viability analysis using the MTT assay revealed that BC-DXI01-mediated cell death was apparent in almost all of the cell lines tested, except for WI-26, H1975, H1972 and H1171 cells (Figure 4B). The susceptibility to BC-DXI01-mediated cell death generally showed a positive correlation with the cellular levels of AIMP2-DX2, apart from some outliers (Figure 4C), suggesting that the apoptotic activity of BC-DXI01 mainly resulted from the suppression of AIMP2-DX2.

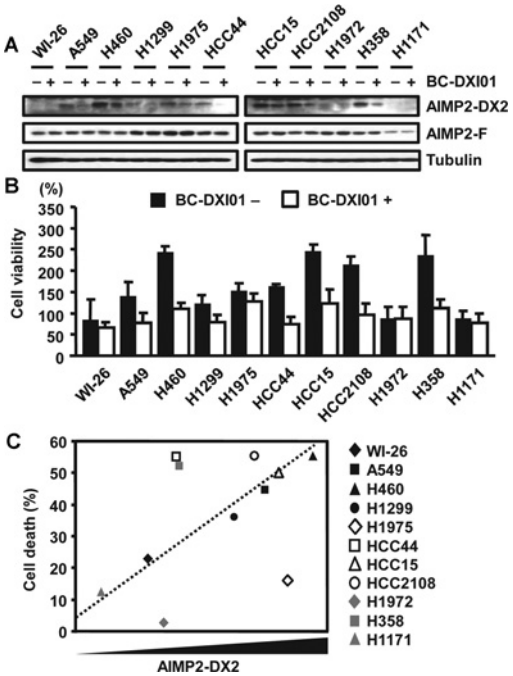

Figure 4 The effect of BC-DXI01 on various NSCLC cell lines

(**A**) WI-26 normal lung cells and other NSCLC cell lines (A549, H460, H1299, H1975, HCC44, HCC15, HCC2108, H1972, H358 and H1171) were treated with BC-DXI01 for 4 h. The effects of BC-DXI01 on the AIMP2-DX2 and AIMP2-F levels in these cell lines were examined using immunoblotting. (**B**) Cell death effects were analysed using the MTT assay after 48 h treatment with BC-DXI01. Results are means ± S.D. and the experiment was repeated three times. (**C**) The level of AIMP2-DX2 protein in each lung cell line was quantified using densitometry. A scatter diagram was plotted to analyse the correlation between BC-DXI01-induced cell death and AIMP2-DX2 levels. The dotted line shows the trend line, which was obtained by ruling out HCC44, H358, H1975 and H1972 cell lines.

Inhibitory effect of BC-DXI01 on tumorigenesis *in vivo*

To test the antitumour activity of BC-DXI01, we established a xenograft mouse model using H460 cells. Since BC-DXI01 did not show good solubility in water, we synthesized a sodium salt form of BC-DXI01 to improve its solubility. The salt form of BC-DXI01 induced degradation of the AIMP2-DX2 transcript with similar efficacy to BC-DXI01 (see Supplementary Figure S4A at http://www.biochemj.org/bj/454/bj4540411add.htm). After once-daily administration of the salt form of BC-DXI01 for 28 days, mice were killed and tumour masses were analysed. Compared with the control group, tumour growth in the BC-DXI01-treated group was apparently inhibited (Figure 5A). Tumour volumes and weights were reduced by up to 60 % following BC-DXI01 treatment (Figures 5B and 5C). However, BC-DXI01 did not affect the body weights of treated mice (see Supplementary Figure S4B). To see whether BC-DXI01 induced cell death in the tumour region, we monitored the activation of caspase 3 in the tumour region by IHC and found a significant increase in apoptotic cells, validating the apoptotic activity of BC-DXI01 *in vivo* (Figure 5D). A decrease in the cellular levels of AIMP2-DX2 and its mRNA transcript was also observed in the BC-DXI01-treated group (see Supplementary Figure S4C). These results suggest that BC-DXI01-mediated AIMP2-DX2 suppression can retard tumour growth *in vivo*.

DISCUSSION

AIMP2 regulates the stability of well-known oncogenes and tumour suppressors via context-dependent protein–protein interactions. AIMP2-DX2 shows increased expression in cancers, and competes with AIMP2 in various signalling pathways to compromise the anti-tumorigenic activity of AIMP2. Thus targeting AIMP2-DX2 could provide an effective therapeutic strategy to treat cancer. In the present study, we performed a screening with 2231 chemical libraries to identify small chemicals that can reduce the levels of AIMP2-DX2 and identified

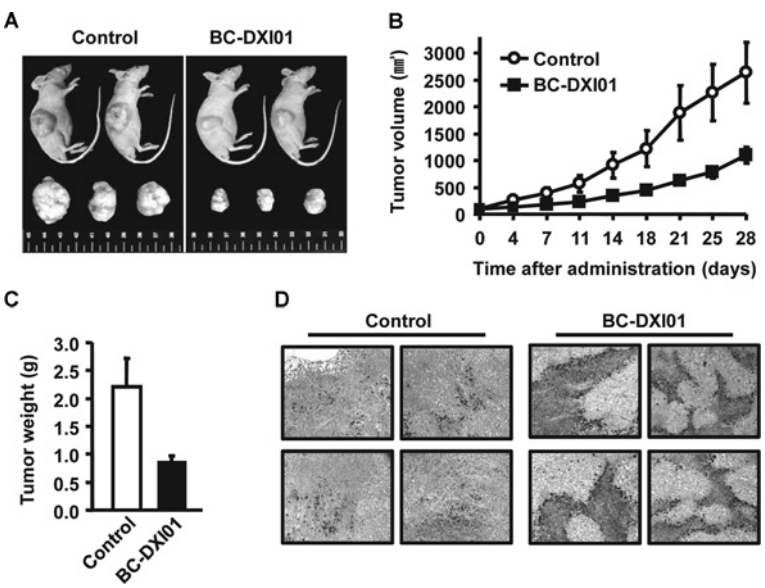

Figure 5 Antitumour activity of BC-DXI01 in a mouse xenograft model

(**A**) Representative photos of control and BC-DXI01-treated mice and their tumour masses are shown. (**B**) Tumour volumes of the two mouse groups ($n = 8$ per group) were measured twice a week. (**C**) Tumour weights of the two mouse groups ($n = 8$ per group) were measured after killing the mice. (**D**) Tumour masses isolated from each group were subjected to IHC staining with anti-(active caspase-3) antibody. Active caspase 3-positive areas are shown in dark grey/black. Results in (**B**) and (**C**) are means ± S.E.M.

BC-DXI01, which has a novel mechanism to reduce the AIMP2-DX2 mRNA transcript, resulting in anti-tumorigenic activity *in vivo*.

By analysing AIMP2-DX2 levels in various NSCLC cell lines, we found that most tested NSCLC cells appear to require AIMP2-DX2 for their survival, except for a few exceptional cases. For instance, the viability of H1975 cells was not significantly affected, although BC-DXI01 treatment successfully suppressed the AIMP2-DX2 level. Perhaps AIMP2-DX2 levels can be also regulated via unknown mechanisms in some cancer cells. The impact of this oncogenic splicing variant on cell survival would need more investigation for better understanding of the AIMP2-DX2 roles in cancer biology.

BC-DXI01 showed specific inhibitory activity to AIMP2-DX2, but not to AIMP2. Interestingly, BC-DXI01 targets the mature mRNA transcript of AIMP2-DX2 and consequently functions as an RNA-interfering chemical molecule. It may induce specific degradation of the AIMP2-DX2 transcript through direct binding to the exon1–3 junction region, although other possibilities can also be considered that could explain the activity of BC-DXI01. The exact mode of action for BC-DXI01 awaits further investigation in molecular detail. Nonetheless, the present study suggests the possibility of chemical-mediated RNA regulation for the development of specific RNA-targeting therapy.

Splicing variants have been recognized as attractive cancer diagnostic markers and drug targets because the controlled switching between splicing variants is closely related to tumour progression [11]. CD44, Wilms' tumour 1, BRCA1/2 (breast cancer early-onset 1/2), PSA (prostate-specific antigen), the kallikrein gene family, MDM2, the fibroblast growth factor receptor family and osteopontin are the representative genes where splicing regulation is linked to their function in various cancers [11,12]. RNA and ribonucleoprotein complexes have received attention as new therapeutic targets, because disruption in their activities has been identified as the cause of numerous diseases [13].

To date, the major obstacle for the development of RNA-regulating therapies lies in the difficulty of delivering antisense oligonucleotides or siRNAs in a tissue-specific manner [13,14]. Chemical-based therapeutics might help overcome this drawback, but, so far, only a few compounds which modulate the spliceosomal proteins or translational machinery have been developed to control alternative splicing of HIV-1 [13,15]. Development of chemicals which can regulate the mature transcript of human mRNA may provide an opportunity for the control of human mRNA without delivery concerns. Optimizing the effects of BC-DXI01 and determining its working mechanism at the molecular level would contribute to the progress in developing pharmaceutical compounds to satisfy the unmet needs in target-based therapy.

AUTHOR CONTRIBUTION

Hee Sook Lee performed the experiments, analysed the data and wrote the paper. Dae Gyu Kim and Young Sun Oh carried out experiments and analysed the data. Nam Hoon Kwon designed and performed the experiments, analysed the data and wrote the paper. Jin Young Lee performed the experiments. Doyeun Kim and Song-Hwa Park performed *in vivo* experiments. Jong-Hwan Song, Sunkyung Lee and Jongkook Lee provided materials. Jung Min Han helped to perform the experiments and analyse the data. Bum-Joon Park helped to design the experiments. Sunghoon Kim designed the experiments, analysed the data and wrote the paper.

Received 19 April 2013/28 June 2013; accepted 1 July 2013
Published as BJ Immediate Publication 1 July 2013, doi:10.1042/BJ20130550

ACKNOWLEDGEMENTS

We thank Dr Young Ho Jeon (Korea University), Dr Ji-Joon Song [KAIST (Korea Advanced Institute of Science and Technology)], Dr Myung Hee Kim [KRIBB (Korea Research Institute of Bioscience and Biotechnology)], Dr Ji-Hyun Lee (Medicinal Bioconvergence Research Center), Dr Key-Sun Kim [KIST (Korea Institute of Science and Technology)] and Dr Jeong-Yong Suh (Seoul National University) for their helpful discussions and suggestions.

FUNDING

This work was supported by the Global Frontier Project [grant numbers NRF-2011-0032185, NRF-2011-0031420 and NRF-M1AXA002-2010-0029785] of the National Research Foundation funded by the Ministry of Education, Science and Technology of Korea. This study was also funded by the Gyeonggi Research Development Program.

REFERENCES

1 Kim, S., You, S. and Hwang, D. (2011) Aminoacyl-tRNA synthetases and tumorigenesis: more than housekeeping. Nat. Rev. Cancer **11**, 708–718
2 Kim, M. J., Park, B. J., Kang, Y. S., Kim, H. J., Park, J. H., Kang, J. W., Lee, S. W., Han, J. M., Lee, H. W. and Kim, S. (2003) Downregulation of FUSE-binding protein and c-myc by tRNA synthetase cofactor p38 is required for lung cell differentiation. Nat. Genet. **34**, 330–336
3 Choi, J. W., Kim, D. G., Park, M. C., Um, J. Y., Han, J. M., Park, S. G., Choi, E. C. and Kim, S. (2009) AIMP2 promotes TNFα-dependent apoptosis via ubiquitin-mediated degradation of TRAF2. J. Cell Sci. **122**, 2710–2715
4 Han, J. M., Park, B. J., Park, S. G., Oh, Y. S., Choi, S. J., Lee, S. W., Hwang, S. K., Chang, S. H., Cho, M. H. and Kim, S. (2008) AIMP2/p38, the scaffold for the multi-tRNA synthetase complex, responds to genotoxic stresses via p53. Proc. Natl. Acad. Sci. U.S.A. **105**, 11206–11211
5 Choi, J. W., Um, J. Y., Kundu, J. K., Surh, Y. J. and Kim, S. (2009) Multidirectional tumor-suppressive activity of AIMP2/p38 and the enhanced susceptibility of AIMP2 heterozygous mice to carcinogenesis. Carcinogenesis **30**, 1638–1644
6 Choi, J. W., Kim, D. G., Lee, A. E., Kim, H. R., Lee, J. Y., Kwon, N. H., Shin, Y. K., Hwang, S. K., Chang, S. H., Cho, M. H. et al. (2011) Cancer-associated splicing variant of tumor suppressor AIMP2/p38: pathological implication in tumorigenesis. PLoS Genet. **7**, e1001351
7 Choi, J. W., Lee, J. W., Kim, J. K., Jeon, H. K., Choi, J. J., Kim, D. G., Kim, B. G., Nam, D. H., Kim, H. J., Yun, S. H. and Kim, S. (2012) Splicing variant of AIMP2 as an effective target against chemoresistant ovarian cancer. J. Mol. Cell Biol. **4**, 164–173
8 Jemal, A., Bray, F., Center, M. M., Ferlay, J., Ward, E. and Forman, D. (2011) Global cancer statistics. Ca-Cancer J. Clin. **61**, 69–90
9 Bunn, Jr, P. A. (2012) Worldwide overview of the current status of lung cancer diagnosis and treatment. Arch. Pathol. Lab. Med. **136**, 1478–1481
10 Bonano, V. I., Oltean, S. and Garcia-Blanco, M. A. (2007) A protocol for imaging alternative splicing regulation *in vivo* using fluorescence reporters in transgenic mice. Nat. Protoc. **2**, 2166–2181
11 Brinkman, B. M. (2004) Splice variants as cancer biomarkers. Clin. Biochem. **37**, 584–594
12 Tilli, T. M., Franco, V. F., Robbs, B. K., Wanderley, J. L., da Silva, F. R., de Mello, K. D., Viola, J. P., Weber, G. F. and Gimba, E. R. (2011) Osteopontin-c splicing isoform contributes to ovarian cancer progression. Mol. Cancer Res. **9**, 280–293
13 Cooper, T. A., Wan, L. and Dreyfuss, G. (2009) RNA and disease. Cell **136**, 777–793
14 Karkare, S. and Bhatnagar, D. (2006) Promising nucleic acid analogs and mimics: characteristic features and applications of PNA, LNA, and morpholino. Appl. Microbiol. Biotechnol. **71**, 575–586
15 Dibrov, S. M., Ding, K., Brunn, N. D., Parker, M. A., Bergdahl, B. M., Wyles, D. L. and Hermann, T. (2012) Structure of a hepatitis C virus RNA domain in complex with a translation inhibitor reveals a binding mode reminiscent of riboswitches. Proc. Natl. Acad. Sci. U.S.A. **109**, 5223–5228

Biochem. J. (2013) **454**, 411–416 (Printed in Great Britain) doi:10.1042/BJ20130550

online data

SUPPLEMENTARY ONLINE DATA

Chemical suppression of an oncogenic splicing variant of AIMP2 induces tumour regression

Hee Sook LEE*[1], Dae Gyu KIM*[1], Young Sun OH*†[1], Nam Hoon KWON*, Jin Young LEE*, Doyeun KIM*, Song-Hwa PARK*, Jong-Hwan SONG‡, Sunkyung LEE‡, Jung Min HAN*, Bum-Joon PARK§, Jongkook LEE‖ and Sunghoon KIM*¶[2]

*Medicinal Bioconvergence Research Center and College of Pharmacy, Seoul National University, Seoul 151-742, Korea, †Department of Biological Science and the Basic Science Research Institute, Sungkyunkwan University, Suwon 440-746, Korea, ‡Bio-Organic Science Division, Korea Research Institute of Chemical Technology, Daejeon 305-343, Korea, §Department of Molecular Biology, College of Natural Science, Pusan National University, Busan 609-735, Korea, ‖College of Pharmacy, Kangwon National University, Chuncheon, Gangwon 200-701, Korea, and ¶Department of Molecular Medicine and Biopharmaceutical Sciences and Graduate School for Convergence Technologies, Seoul National University, Seoul 151-742, Korea

EXPERIMENTAL

Cell culture

WI-26, a human embryonic lung fibroblast cell line, was obtained from the Korea Cell Line Bank. The other NSCLC cell lines, A549, H460, H1299, H1975, HCC44, HCC15, HCC2108, H1972, H358 and H1171, were purchased from A.T.C.C. (Manassas, VA, U.S.A). Cell lines were maintained in DMEM (Dulbecco's modified Eagle's medium) (WI-26 cells) or RPMI 1640 (other NSCLC cell lines) medium complemented with 10 % FBS and 1 % penicillin/streptomycin and kept in a 5 % CO_2 incubator at 37 °C. For chemical treatment, cells were incubated with compounds in serum-free or 0.5 % serum-containing medium for the indicated times. H460 cell lines were pre-incubated with actinomycin D (Sigma) for 4 h before being treated with BC-DXI01 to see the effect of BC-DXI01 under the condition of transcriptional inhibition.

Northern blotting

Total RNA was isolated from BC-DXI01-treated H460 cells using TRIzol®, and 50 μg of RNA was separated by agarose gel electrophoresis and then transferred to Hi-bond membranes (Amersham). After baking for 2 h at 80 °C, the membrane was processed using a Brightstar biodetect nonisotopic detection kit (Ambion) following the manufacturer's guidelines. To generate a DNA probe for AIMP2-DX2, PCR was performed with the primer pair 5′-ATGCCGATGTACCAGGTAAAG-3′ (forward) and 5′-GTTTTCAGGCACGCTCTTGACCGAG-3′ (reverse) and then the PCR product (284 bp) was conjugated with biotin as suggested in the BrightStar psoralen-biotin nonisotopic labelling kit (Ambion).

Immunoblotting

Cell lines treated with compounds were harvested at the times indicated. The cells were lysed with lysis buffer containing 50 mM Tris/HCl, pH 7.4, 150 mM NaCl, 0.5 % Triton X-100, 5 mM EDTA, 10 % glycerol and protease inhibitors (Calbiochem). Frozen tumour tissues were homogenized in the lysis buffer. The lysates were centrifuged at 10000 **g** for 30 min at 4 °C to obtain the supernatant and the protein concentration was determined using a Bio-Rad protein assay kit. For immunoblotting, 50 μg of protein lysate per sample was subjected to SDS/PAGE after being mixed with SDS/PAGE sample buffer and then transferred on to a PVDF membrane. The PVDF membrane was blocked with 5 % (w/v) non-fat dried skimmed milk powder in TBST (10 mM Tris, pH 7.4, 10 mM NaCl and 0.1 % Tween 20), incubated with the primary antibody overnight at 4 °C, and the bound antibodies were detected with a HRP (horseradish peroxidase)-labelled secondary antibody using West-one™ solution (iNtRON, Korea). The monoclonal antibody recognizing both AIMP2-F and AIMP2-DX2 was purchased from Neomics (Korea), and anti-PARP-1 and anti-actin antibodies were obtained from Santa Cruz Biotechnology. Anti-tubulin antibody was purchased from Sigma.

MTT assay

H460 cells (1×10^4 cells) were seeded in 96-well plates and treated with compounds for the indicated times in 0.5 % serum-containing medium. MTT (USB) stock solution (5 mg/ml) was 10-fold diluted and 10 μl of diluted solution was added to each well containing 200 μl of medium and incubated for 30 min. The precipitated crystal was dissolved in 100 μl of DMSO (Sigma). Absorbance was measured at 420 nm using a microplate reader (Sunrise, TECAN).

Flow cytometry

H460 cells were treated with BC-DXI01 (0.04, 0.4 and 4 μM) in 0.5 % serum-containing medium for 48 h. The treated cells were fixed with 70 % ethanol for 1 h at 4 °C, washed twice with ice-cold PBS, and stained with propidium iodide (50 μg/ml) containing 0.1 % sodium citrate, 0.3 % Nonidet P40 and 50 μg/ml RNase A for 40 min. The cells were subjected to flow cytometry (FACSCalibur, Becton-Dickinson) to evaluate the apoptotic cells by counting the sub-G_1 cells. For each sample, 20000 cells were analysed using Cell Quest Pro software.

Thymidine incorporation assay

H460 cells were treated with BC-DXI01 (0.04, 0.4 and 4 μM) in 0.5 % serum-containing medium for 48 h. [^{3}H]Thymidine at 1 μCi/ml was added to the culture medium and was incubated for 4 h. The incorporated thymidine was measured using a liquid scintillation counter (Wallac).

IHC

Dissected tumours were fixed and stored in 10 % neutral-buffered formalin. Tissues were processed, paraffin-embedded,

[1] These authors contributed equally to this work.
[2] To whom correspondence should be addressed (email sungkim@snu.ac.kr).

and sectioned at 6 μm thickness. After deparaffinization, antigen retrieval was performed by boiling sections for 5 min in sodium citrate solution (0.01 M, pH 6). Sections were incubated at 4 °C overnight with rabbit anti-(active caspase 3) antibody (1:200 dilution, Cell Signaling Technology) in PBST (0.3 % Triton X-100 in PBS) containing 5 % goat serum. After washing, sections were incubated with biotin-conjugated anti-(rabbit IgG) (1:100 dilution, Sigma) antibody and ExtrAvidin-peroxidase (1:50 dilution, Sigma) at room temperature for 1 h each. Sections were developed with DAB (3, 3-diaminobenzidine) substrate for 30 min, counterstained with haematoxylin and imaged under the microscope.

In vitro transcription

To generate RNA fragments of AIMP2 and AIMP2-DX2 transcripts, PCR was performed with specific primers. A common forward primer with a T7 promoter sequence, 5′-TAATACGACTCACTATAATGCCGATGTACCAGGTAAAG-3′, was used for every reaction in combination with each reverse primer. Specific reverse primers, 5′-TGGGGAGCCGGTACATGCAGGTGGG-3′, 5′-GGGGAGGCCGGGTTTGCGTTGATCA-3′, 5′-GTTTTCAGGCACGCTCTTGACCGAG-3′, 5′-GTTGCGTTGACAGCATTATGCTTCT-3′, 5′-TCACTTAAGGAGCTTGAGGGCCGTGTTAAA-3′ and 5′-ATTCTTCCAAATTAAAGTGAATCCC-3′, were used for the amplification of DX2-f85, DX2-f185, DX2-f285, DX2-f485, DX2-full and AIMP2-f573 respectively. Amplified PCR products were purified and RNA was synthesized by *in vitro* transcription using each PCR template and T7 RNA polymerase (Promega). For the filter-binding assay, RNA was radioactively labelled using [α-^{32}P]UTP.

Filter-binding assay (dot blot assay)

Biotinylated BC-DXI01 and radioactively labelled RNA (10000 c.p.m.) were incubated in the binding buffer (20 mM Tris/HCl, pH 7.4, 75 mM KCl, 10 mM $MgCl_2$ and 5 % glycerol) at room temperature for 30 min. The reaction mixtures were filtered through a streptavidin-coated matrix biotin-capture membrane (Promega) using a 96-well Minifold filtration apparatus. Dried membranes were exposed, and signals were detected by autoradiography.

Pull-down assay for BC-DXI01 and RNA complex

Synthesized RNA fragments (2 μg) were added to the biotinylated BC-DXI01 in the RNA-binding buffer (200 mM KCl, 20 mM NaCl, 0.05 % Nonidet P40, 10 % glycerol, 2 mM DTT, 2 mM $MgCl_2$ and 20 mM Hepes, pH 7.8), and incubated for 1 h at 30 °C. After cross-linking by the addition of 1 % formaldehyde at room temperature for 10 min, the RNA–BC-DXI01 complex was pulled down using streptavidin–Sepharose beads (1 h incubation with rotation). After washing and incubation with DNase I (Fermentas) to remove contaminating DNA, RNA was extracted with phenol/chloroform and precipitated by ethanol. Each RNA fragment was detected via RT–PCR using a common forward primer, 5′-ATGCCGATGTACCAGGTAAAG-3′, and the specific reverse primer described in the *In vitro* transcription section above.

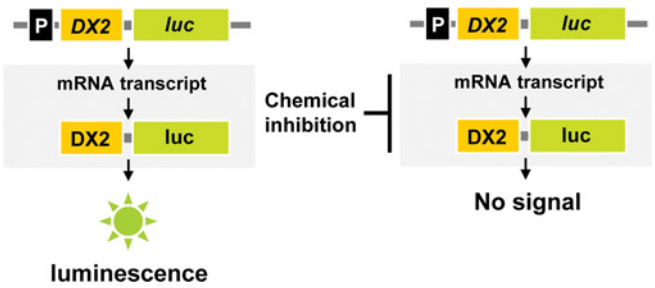

Figure S1 Schematic diagram for the chemical screening based on luciferase assay

AIMP2-DX2 was cloned into the pGL2 control vector, fused to the 5′ end of firefly luciferase and expressed in H460 cells. The protein level of AIMP2-DX2 was monitored by luminescence (left-hand panel). When chemicals inhibit the expression of AIMP2-DX2 at the mRNA or protein level, luciferase activity is decreased and the efficacy of compounds can be calculated (right-hand panel). P, promoter.

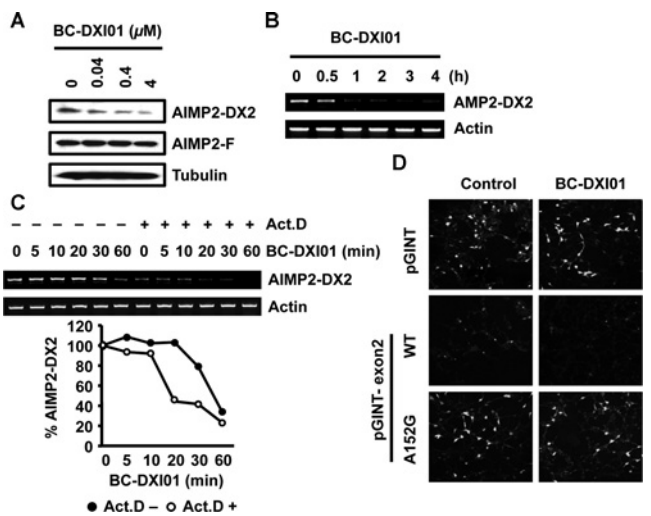

Figure S2 BC-DXI01 induces degradation of the AIMP2-DX2 transcript without affecting the splicing process

(**A**) BC-DXI01 was treated to H460 cells for 4 h and the amounts of AIMP2-DX2 and AIMP2-F were detected by immunoblotting. (**B**) The effect of BC-DXI01 (0.4 μM) on the mRNA transcript levels was monitored at early time points via RT–PCR. (**C**) H460 cells were pre-incubated with actinomycin D (Act.D, 2 μM) for 4 h and then treated with BC-DXI01 for the indicated time periods. The mRNA level of AIMP2-DX2 was examined via RT–PCR (upper panel). The band intensity of AIMP2-DX2 was measured and the relative percentage of AIMP2-DX2 mRNA is presented (lower panel). (**D**) pGINT, pGINT-exon2 wild-type (WT) or pGINT-exon2 A152G mutant were transfected into H460 cells and incubated with DMSO (control) or BC-DXI01. Expression of GFP was monitored using fluorescence microscopy.

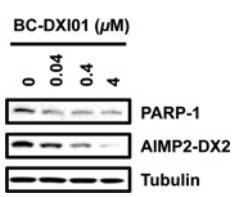

Figure S3 BC-DXI01 induces apoptosis of H460 lung cancer cells

H460 cells were treated with the indicated concentrations of BC-DXI01 for 48 h. Expression of AIMP2-DX2 and PARP-1 was analysed via immunoblotting.

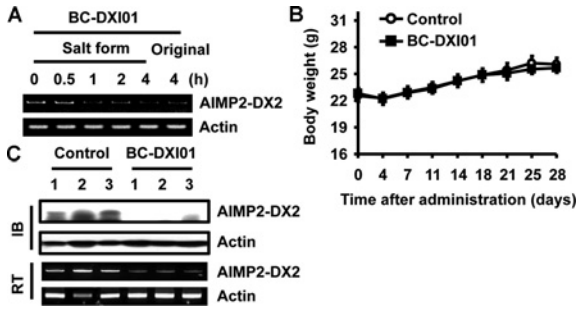

Figure S4 Antitumour activity of BC-DXI01 in a mouse xenograft model

(**A**) H460 cells were treated with the sodium salt form of BC-DXI01 and the mRNA level of AIMP2-DX2 was analysed using RT–PCR. Original BC-DXI01 was used as a positive control. (**B**) Body weights of mice administered with the BC-DXI01 salt form or vehicle were measured twice a week. Results are means$\pm$S.D. ($n = 8$ per group). (**C**) Protein and mRNA levels of AIMP2-DX2 were analysed from the tumours and the results are presented. IB, immunoblot; RT, RT–PCR.

Received 19 April 2013/28 June 2013; accepted 1 July 2013
Published as BJ Immediate Publication 1 July 2013, doi:10.1042/BJ20130550